Preparation and photocatalytic activity of nanoglued Sn-doped TiO$_2$

Xiang Li, Rongchun Xiong, Gang Wei*

College of Materials Science and Engineering, Beijing University of Chemical Technology, Beisanhuan Donglu 15#, 100029 Beijing, China

ABSTRACT

In this paper, Sn-doped TiO$_2$ photocatalyst was prepared and immobilized on a glass substrate using an about-to-gel SiO$_2$ sol as a nanoglue. The characterization of the Sn-doped TiO$_2$ by XRD showed that 5% Sn content is formed by anatase and rutile crystallites. Characterization of the nanoglued photocatalyst by the BET measurement, TEM, and SEM showed that the photocatalyst was a nanoporous material with a high-surface area. The Sn-doped TiO$_2$ was uniformly dispersed within the three-dimensional network of the silica in the form of nanoparticles. The nanoglued photocatalyst showed high photocatalytic activity during the degradation of penicillin under UV light. The effect of different Sn content on the amount of hydroxyl radical was discussed by using salicylic acid as probe molecules. The results show that an appropriate amount of Sn dopant can greatly increase the amount of hydroxyl radicals generated by TiO$_2$ nanoparticles, which are responsible for the obvious increase of photocatalytic activity.

© 2008 Elsevier B.V. All rights reserved.

1. Introduction

TiO$_2$ has been widely used as a photocatalyst in waste air and wastewater treatment due to its relatively high photocatalytic activity, chemical stability, nontoxicity, low cost, and resistance to chemical pollutants [1–5]. However, the fast recombination rate of photogenerated electron/hole pairs hinders the commercialization of this technology. According to recent research, composite semiconductors could be an effective method because they may increase the efficiency of charge separation and extend the energy range of photoexcitation. In the past several years, there have been a number of studies related to TiO$_2$ coupled with a metal oxide like SnO$_2$ [6,7], WO$_3$ [8,9], ZnO [10], Fe$_2$O$_3$ [11,12]. Among them, coupling TiO$_2$ with SnO$_2$ could remarkably increase photocatalytic activity, because the electronic energy levels of these two substances match. However, the recovery/reuse of the catalyst needs to be solved prior to the application of TiO$_2$ photocatalyst. For better recovery and reuse, TiO$_2$ can be prepared in immobilized forms. A sol–gel method was employed by Zhang and coworkers [13,14] to prepare TiO$_2$/glass photocatalyst which can degrade Rhodamine B effectively. Lee et al. [15] prepared high quality films using MOCVD. However, this kind of method to immobilize TiO$_2$ particles cannot be widely applied because of the complicated preparation procedure.

In this paper, nanoglued Sn-doped TiO$_2$ was prepared using silica gel as a "nanoglue" [16,17]. The photocatalyst was dispersed in the silica network which makes it possible for it to possess a large specific surface area and a high porosity. The SnO$_2$ improved the charge transfer of the TiO$_2$ and the recovery problem of the catalyst was alleviated by immobilizing it onto a glass. The photocatalytic activity was evaluated by degradation of penicillin solution since penicillin was the main pollutant of antibiotic wastewater.

2. Materials and methods

2.1. Preparation of Sn-doped TiO$_2$ nanoparticles

According to Refs. [13,14], the sol–gel method was adopted to prepare TiO$_2$ sol. A mixture of 5 ml distilled H$_2$O and 10 ml ethanol (AR) was added dropwise at room temperature to a mixture of 5 ml Ti(OC$_4$H$_9$)$_4$(AR) and 15 ml ethanol. Subsequently, the yellowish transparent sol was yielded after continuously stirring for 2 h. After the sol was allowed to stand for 24 h at room temperature, the TiO$_2$ xerogel was obtained. Finally, TiO$_2$ nanoparticles were gained by calcining the TiO$_2$ xerogel at 450 °C for 2 h and grinding.

A different content of Sn-doped TiO$_2$ nanoparticles can be obtained by repeating the same step while replacing H$_2$O as a specified concentration solution of SnCl$_4$. The Sn content were 0, 1, 2, 3, 4, 5 mol.%, and the obtained powders were labeled as SnTiO$_2$0, SnTiO$_2$1, SnTiO$_2$2, SnTiO$_2$3, SnTiO$_2$4, SnTiO$_2$5.

* Corresponding author. Tel.: +86 10 64455013; fax: +86 10 64416221.
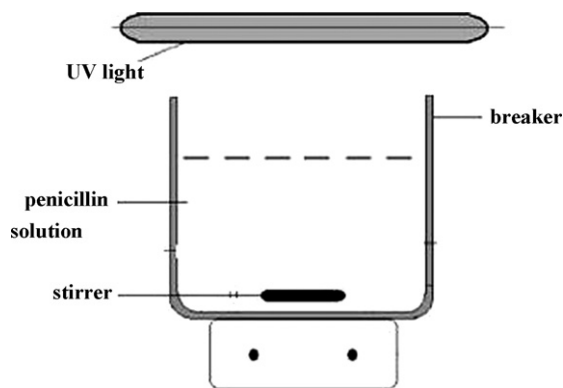*E-mail address:* weigangmail@263.net (G. Wei).

Fig. 1. Photocatalytic experimental setup for degradation of penicillin.

2.2. Preparation of nanoglued Sn-doped TiO$_2$

The silica sol was prepared according to the following method: tetraethoxysilane (TEOS), ethanol, and water (molar ratio TEOS/H$_2$O/C$_2$H$_5$OH 1:5:10) were mixed under vigorous stirring; aqueous ammonia (20 wt.%) were dropped into the mixed solution to make pH to 9. After stirring for 3 h, the solution became transparent, and then, it was deposited at room temperature for 24 h.

The microscope slides (made of ordinary glass) were dipped into 1 M NaOH solution for 24 h. Afterwards, each slide was rinsed using distilled water. The nanoglued photocatalyst was immobilized by the brushing method. A certain weight of nano-TiO$_2$ powder was added into a 20 ml SiO$_2$ sol. A brush was used to coat both sides of the slide after the mixture was ultrasonically dispersed for 30 min. After being dried using a blow dryer, the sample was heated to 150 °C for 30 min in an air flow oven. The thickness of the film was adjusted by repeating the same process.

2.3. Characterization of photocatalyst

The prepared Sn-doped TiO$_2$ nanoparticles were characterized by X-ray diffraction (XRD, XRD-6000, Shimadzu, Japan) using a Cu Kα radiation source (λ = 0.154056 nm) at 30 kV, with a scanning rate of 5°/min. The nanoglued photocatalysts were characterized by a scanning electronic microscope (SEM, S-4700, Hitachi, Japan) and a high-resolution transmission electron microscope (HRTEM, JEOL-2011). The Brunauer–Emmett–Teller (BET) surface area of the photocatalyst was obtained from nitrogen adsorption–desorption data (Quanta chrome Autosorb-1 system). To investigate the light absorption properties of Sn-doped TiO$_2$, UV–vis absorption spectra were obtained using a UV–vis spectrophotometer (UV 2550, Shimadzu, Japan). Pure BaSO$_4$ was used as a reflectance standard in the UV–vis absorbance experiment.

2.4. Photocatalytic degradation of penicillin solution

The photocatalytic degradation of penicillin was conducted in a quartz reactor, as shown in Fig. 1. About 0.1 g nanoglued photocatalyst was put into a beaker containing 100 ml of penicillin solution with an initial COD of 300 mg/l. The light was provided by a 36W black light lamp without filter, which was placed about 15 cm from the side of the reactor, its strongest emission light having the wavelength of 365 nm. The penicillin solution was continuously stirred with a magnetic stirrer. At a certain time interval, the COD of the sample was measured on a Hach COD analysis apparatus. The degradation rate of penicillin was calculated based on the following
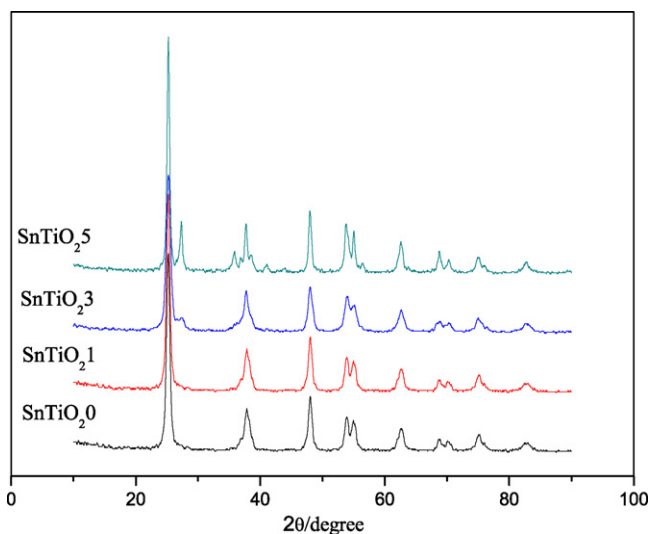

Fig. 2. XRD patterns of TiO$_2$ with different Sn dopant amounts of nanoparticles calcined at 450 °C.

formula:

$$\eta = \frac{(COD_0 - COD)}{COD_0} \qquad (1)$$

where η stands for the photocatalytic degradation rate of penicillin; while COD_0 and COD stand for the initial and final COD value, respectively. In order to evaluate the absorbance of penicillin by nanoglued photocatalyst, experiment was run under the same condition but without UV irradiation. The degradation rate of penicillin was calculated based on the same formula (1).

2.5. Measurement of hydroxyl radical

During the photocatalysis process, hydroxyl radicals have been regarded as the major species for the mineralization of pollutants. The degradation of penicillin has also been assumed to follow the reaction mechanism of hydroxyl oxidation. According to Ref. [18], salicylic acid was used as probe molecules to validate the appearance of hydroxyl radicals in the photocatalytic degradation of penicillin with our nanoglued Sn-doped TiO$_2$. The salicylic acid reacted with the hydroxyl radicals to form 2,3-dihydroxybenzoic acid. After reacting 1 h, the amounts of hydroxyl radicals absorbed by the solution at the wavelength of 510 nm were measured. A blank experiment was run before adding the photocatalyst. There was no change in the absorbance, which indicated that there was no photolysis reaction in salicylic acid under UV irradiation.

3. Results and discussion

3.1. Characterization of Sn-doped TiO$_2$ nanoparticle

Fig. 2 shows XRD patterns for synthesized TiO$_2$ powders calcined at 450 °C with different Sn content. The phase composition varies with the increasing content of Sn. The XRD peaks at $2\theta = 25.28°$ (1 0 1) and $2\theta = 27.4°$ (1 1 0) are often taken as the characteristic peaks of anatase and rutile crystal phase, respectively. According to the XRD patterns, the pure TiO$_2$ sample constituted pure anatase phase, in accordance with other TiO$_2$ photocatalysts obtained by the same crystallization route from different precursors [4]. On the other hand, the sample containing Sn shows a multiphase composition as the Sn content increases. The 5 mol.% Sn sample is composed of crystallites of both anatase and rutile phase. The formation
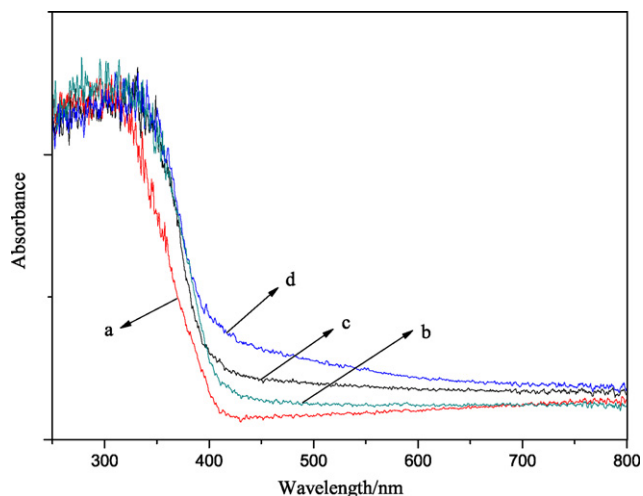
Fig. 3. UV–vis spectra of Sn-doped TiO$_2$ with different concentrations and calcined at 450 °C (a: 0%; b: 1%; c: 3%; d: 5%).

of crystallites of rutile phase at a low calcination temperature is induced by the presence of Sn, as previously reported [19,20]. No SnO$_2$ phase is detected, which suggests the incorporation of Sn^{4+} into the TiO$_2$ lattice [19].

UV–vis absorption spectra of Sn-doped TiO$_2$ of different Sn content are presented in Fig. 3. It can be seen that the Sn-doped TiO$_2$ showed stronger light absorption property in the UV region and further slightly red-shifted to the visible-light region. The red shift can be attributed to the charge-transfer transitions between doped Sn^{4+} electrons and the TiO$_2$ conduction band [21]. It is known that the process for photocatalysis of semiconductors is the direct absorption of a photon by band gap of the material and generates electron-hole pairs in the semiconductor particles. The extended absorbance of Sn-doped TiO$_2$ photocatalyst provides a possibility for enhancing the photocatalytic performance of TiO$_2$.

3.2. Characterization of nanoglued photocatalyst

Fig. 4a and b shows the TEM images of the nanoglued photocatalyst. Titanium dioxide is presented as sphere particles uniformly dispersed in the silica xerogel network. Titanium dioxide nanoparticles were surrounded by amorphous silica which paved the way for the photocatalyst to have a large specific surface area. The nitrogen sorption isotherm measurement shows that the nanoglued photocatalyst has a typical type IV adsorption and a large surface area of 399 m^2/g while the pure TiO$_2$ nanoparticles have only 134 m^2/g. While the silica gel was being deposited, a three-dimensional (3D) network of SiO$_2$ particles had been formed. After the introduction of TiO$_2$, the nanoparticles were dispersed in the network, which made it possible for the nanoglued photocatalyst to keep a high specific surface area and a high porosity. The resistance to mass transfer of photocatalytic reaction is low and the reactant easily gets in contact with the catalytic active site.

Fig. 5a and b shows the nanoglued photocatalyst on a glass. It can be seen from Fig. 5a that the particles are highly dispersed and that the amorphous SiO$_2$ is porous. When TiO$_2$ particles were dispersed in the silica gel network, the silica was able to confine the agglomeration and motion of the particles. Meanwhile, the size and morphology of the nanoparticles remained at the same size before being dispersed. As can be seen in Fig. 5b, when titanium dioxide nanoparticles in silica got in contact with the outside environment, a high photocatalytic activity was ensured.
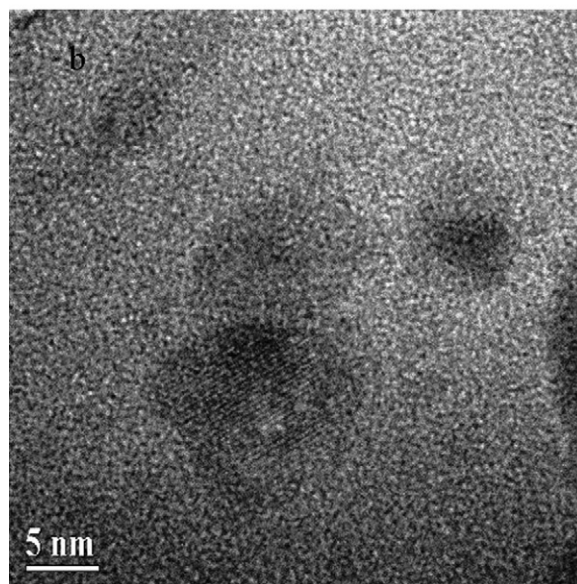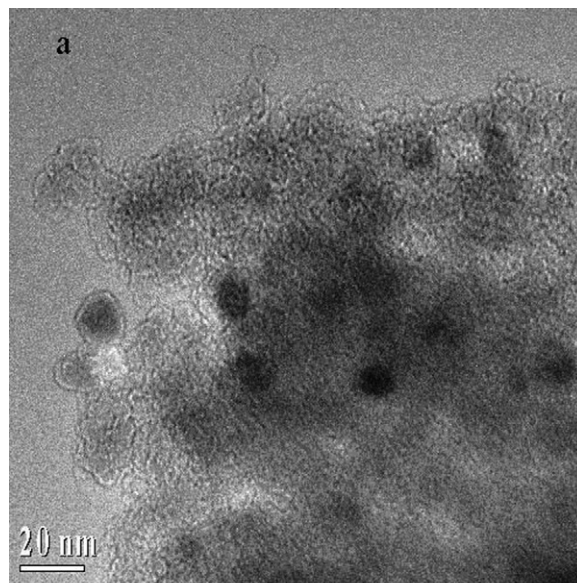

Fig. 4. (a and b) TEM images of nanoglued photocatalyst.

3.3. Effects of Sn content on hydroxyl radicals

When TiO$_2$ was illuminated by ultraviolet light, the following reaction took place on the surface of the photocatalyst.

$$TiO_2 \xrightarrow{h\nu} e^- + h^+ \tag{2}$$

$$h^+ + H_2O \rightarrow {}^\bullet OH + H^+ \tag{3}$$

$$h^+ + OH^- \rightarrow {}^\bullet OH \tag{4}$$

$$h^+ + e^- \rightarrow N + energy \tag{5}$$

The OH$^-$ and H$_2$O which were absorbed on the surface of TiO$_2$ will be oxidized into hydroxyl radicals by photogenerated holes. Pollutants in the water can be degraded into H$_2$O and CO$_2$ by hydroxyl radicals. However, at the same time, photogenerated electron and holes can be recombined quickly. Thus, the amounts of hydroxyl radicals and the efficient charge separation directly influenced the photocatalytic activity.
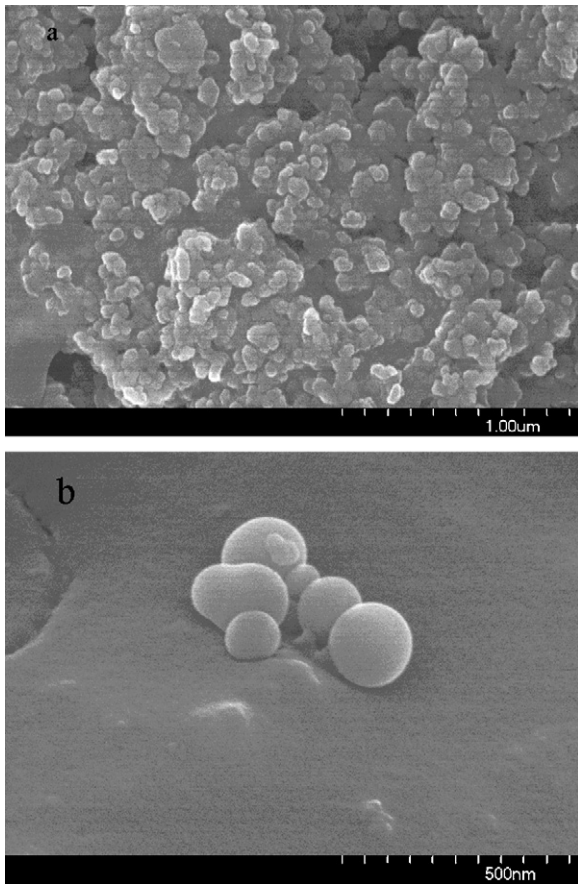
Fig. 5. (a and b) SEM image film of nanoglued photocatalyst.

Fig. 6 shows the hydroxyl radical with different Sn content calcined at 450 °C. It can be seen that Sn-doped TiO$_2$ generated more hydroxyl radicals than pure TiO$_2$. This is because photoinduced electrons easily transfer from TiO$_2$ to SnO$_2$ due to their potential difference of conduction band. According to Ref. [22], the conduction band (CB) edges of TiO$_2$ and SnO$_2$ are situated at −0.34 and +0.07 V versus normal hydrogen electrode (NHE) at pH 7. Thus, electron can easily flow into SnO$_2$, which has a more positive conduction band.
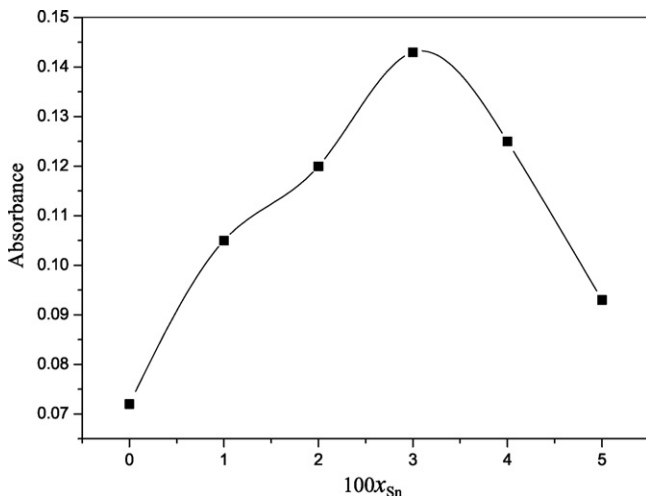

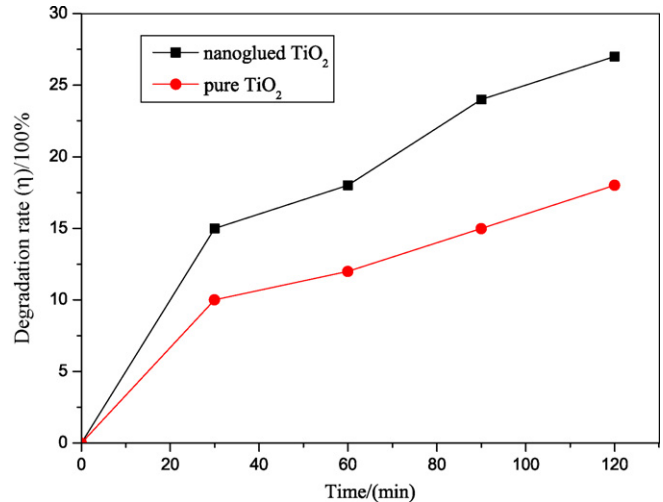**Fig. 6.** Hydroxyl radical amounts on Sn-doped TiO$_2$ with different Sn content.

Fig. 7. Degradation rate of nanoglued TiO$_2$ and pure TiO$_2$ under dark condition.

This results into the decrease in the chance of recombination of photoinduced carriers so that the separation rate of photoinduced electron-hole pairs can improve, that is, the amount of hydroxyl radicals can increase. The Sn content has a great effect on the hydroxyl radicals of TiO$_2$. The amount of hydroxyl radicals increases as the Sn content increases. As can be seen in Fig. 6, the hydroxyl radical of TiO$_2$ doped with 3 mol.% Sn is very high, indicating that the sample has a high separation rate of photoinduced carriers. However, the amount of hydroxyl radicals can decrease if the Sn content is too high. There are two possible reasons for this. One reason is that the amount of photoinduced electrons accumulating instantly at the SnO$_2$ conduction band is too much due to excess SnO$_2$ so that some photoelectrons can indirectly recombine with holes. The second is that an excess amount of Sn dopant can produce the recombination center of photoinduced electron and hole pairs. Therefore, it can be concluded that an appropriate amount of Sn dopant can increase the amount of hydroxyl radicals. In other words, the separation rate of photoinduced charge carriers can be improved by doping an appropriate amount of Sn.

3.4. Photocatalytic degradation of penicillin using nanoglued Sn-doped TiO$_2$

To evaluate the absorption ability of nanoglued sample, degradation of penicillin solution was run under dark condition which is graphically illustrated in Fig. 7. From the figure, it is clear that degradation of penicillin of nanoglued sample is faster than pure TiO$_2$ powders. This can be attributed to the high porosity of the nanoglued sample, which correlates to a strong adsorption ability.

Fig. 8 reflects the photocatalytic activity of nanoglued photocatalysts with different Sn content. The experiment results indicate that the photocatalytic activity of nanoglued photocatalyst can be improved by doping an appropriate content of Sn. When the Sn content is 3 mol.%, the photocatalyst exhibits higher photocatalytic activity. If the Sn content continuously increases, the photocatalytic activity begins to fall down inversely. Moreover, the order of the photocatalytic activity of different nanoglued photocatalysts can be reasonably explained by means of hydroxyl radical determination.

The photoinduced holes which generated hydroxyl radicals are mainly used to oxidize organic pollutants during the process of photocatalytic reaction. In general, the more positive the valence
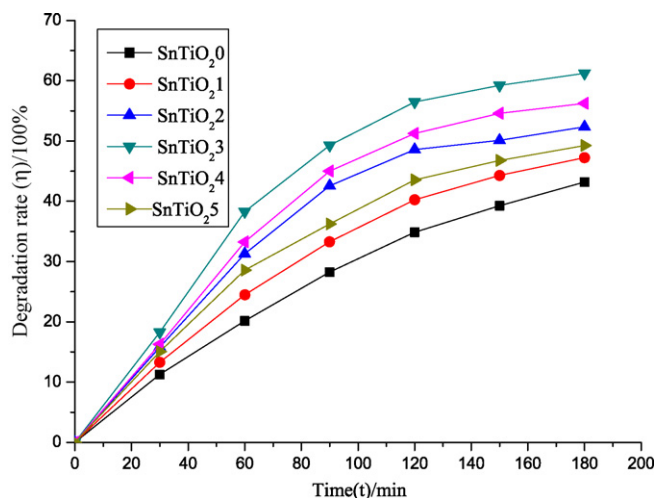
Fig. 8. Influence of Sn content on the photocatalytic activity of nanoglued photocatalysts.

band potential, the stronger the oxidation capability of photoinduced holes, which favors the increase of photocatalytic activity. The higher the separation rates of photoinduced carriers, the higher the photocatalytic activity [1,2]. Among different Sn content photocatalysts, the 3 mol.% Sn content exhibits more hydroxyl radicals, indicating that the separation rate of photoinduced carriers is higher, which is responsible for the higher photocatalytic activity.

The oxidation capability of the photoinduced holes of SnO_2 is stronger than that of TiO_2 since the valence band position of SnO_2 is lower than that of TiO_2. However, the band gap of SnO_2 is wide ($E_g = 3.6$ eV) so that only the light at a wavelength lower than 345 nm can be used to excite SnO_2. In our photocatalytic degradation experiment, a black light lamp is used as the light source, and its strongest emission light is at the wavelength of 365 nm. Therefore, most of the photoinduced holes of nanoglued Sn-doped TiO_2 sample mainly result from TiO_2 other than SnO_2. However, doping an appropriate amount of Sn can effectively enhance the separation rates of photoinduced carriers of TiO_2, which has been proved by hydroxyl radical measurements. This is responsible for the increase in the activity of photocatalysts.

4. Conclusions

A nanoglued photocatalyst was prepared using the technique of nanogluing Sn-doped TiO_2 powders into a three-dimensional network of silica sol. The nanoglued photocatalyst showed to have a high-surface area and strong absorbency, which increase the concentration of penicillin near the TiO_2 sites, thus enhancing the destruction efficiency. The effect of Sn dopant on the photoinduced charge property was estimated by measuring hydroxyl radicals using salicylic acid as probe molecules. The results show that doping an appropriate amount of Sn can improve the photocatalytic activity of TiO_2 by enhancing the separation rate of the photoinduced charge carriers of TiO_2.

References

[1] M.R. Hoffmann, S.T. Martin, W.Y. Choi, D.W. Bahnemann, Environmental applications of semiconductor photocatalysis, Chem. Rev. 95 (1) (1995) 69–96.
[2] A.L. Linsebigler, G.Q. Lu, J.T. Yates Jr., Photocatalysis on TiO_2 surfaces principles, mechanisms, and selected results, Chem. Rev. 95 (3) (1995) 735.
[3] N. Negishi, T. Iyoda, K. Hashimoto, A. Fujishima, Preparation of transparent TiO_2 thin film photocatalyst and its photocatalytic activity, Chem. Lett. 24 (9) (1995) 841–843.
[4] I. Sopyan, M. Watanabe, S. Murasawa, Efficient TiO_2 powder and film photocatalysts with rutile crystal structure, Chem. Lett. 1 (1996) 69–71.
[5] T. Torimoto, S. Ito, S. Kuwabata, H. Yoneyama, Effects of adsorbents used as supports for titanium dioxide loading on photocatalytic degradation of propyzamide, Environ. Sci. Technol. 30 (1996) 1275–1281.
[6] K. Tennakone, J. Bandara, Photocatalytic activity of dye-sensitized tin(IV) oxide nanocrystalline particles attached to zinc oxide particles: long distance electron transfer via ballistic transport of electrons across nanocrystallites, Appl. Catal. A Gen. 208 (2001) 335–341.
[7] J. Lin, J.C. Yu, D. Lo, S.K. Lam, Photocatalytic activity of rutile $Ti_{1-x}Sn_xO_2$ solid solutions, J. Catal. 183 (1999) 368–372.
[8] T. Ohno, T. Tanigawa, K. Fujihara, S. Izumi, M. Matsumura, Photocatalytic oxidation of water on TiO_2-coated WO_3 particles by visible light using Iron(III) ions as electron acceptor, J. Photochem. Photobiol. A Chem. 118 (1998) 41–44.
[9] X.Z. Li, F.B. Li, C.L. Yang, W.K. Ge, Photocatalytic activity of WO_x–TiO_2 under visible light irradiation, J. Photochem. Photobiol. A Chem. 141 (2001) 209–217.
[10] C. Wang, J.C. Zhao, X.M. Wang, B.X. Mai, G.Y. Sheng, P.J. Peng, J.M. Fu, Preparation, characterization and photocatalytic activity of nano-sized ZnO/SnO_2 coupled photocatalysts, Appl. Catal. B Environ. 39 (2002) 269–279.
[11] B. Pal, M. Sharon, G. Nogami, Preparation and characterization of TiO_2/Fe_2O_3 binary mixed oxides and its photocatalytic properties, Mater. Chem. Phys. 59 (1999) 254–261.
[12] B. Pal, T. Hata, K. Goto, G. Nogami, Photocatalytic degradation of o-cresol sensitized by iron–titania binary photocatalysts, J. Mol. Catal. A Chem. 169 (2001) 147–155.
[13] G. Wei, Y.J. Zhang, R.C. Xiong, Controllable preparation of nanosized TiO_2 thin film and relationship between structure of film and its photocatalytic activity, Sci. China (Series B) 46 (2003) 184–191.
[14] G. Wei, Y.J. Zhang, R.C. Xiong, Photocatalysis degradation kinetics of Rhodamine B using TiO_2, Chin. Sci. Bull. 47 (2002) 1793–1795.
[15] J.S. Lee, H.W. Song, W.J. Lee, et al., Effects of process parameters on titanium dioxide thin film deposited using ECR MOCVD, Thin Solid Films 287 (1996) 120–124.
[16] M.L. Anderson, C.A. Morris, R.M. Stroud, C.I. Merzbacher, D.R. Rolison, Colloidal gold aerogels: preparation, properties, and characterization, Langmuir 15 (1999) 674–681.
[17] C.A. Morris, M.L. Anderson, R.M. Stroud, D.R. Rolison, C.I. Merzbrcher, Silica sol as a nanoglue: flexible synthesis of composite aerogels, Science 284 (1999) 622–624.
[18] R.C. Xiong, C.G. Jia, G. Wei, Treatment of dyestuffs wastewater with two and three-dimension electrode methods, J. BUCT (Nature Science Edition) 29 (2002) 34–37.
[19] F. Fresno, J.M. Coronado, D. Tudela, J. Soria, Influence of the structural characteristics of $Ti_{1-x}Sn_xO_2$ nanoparticles on their photocatalytic activity for the elimination of methylcyclohexane vapors, Appl. Catal. B: Environ. 55 (2005) 159–167.
[20] K.N.P. Kumar, K. Keizer, A.J. Burgraaf, T. Okubo, J. Nagamoto, Synthesis and textural properties of unsupported and supported rutile (TiO_2) membranes, J. Mater. Chem. 3 (1993) 923–929.
[21] E. Arpaç, F. Sayılkan, M. Asiltürk, P. Tatar, N. Kiraz, SayılkanF H., Photocatalytic performance of Sn-doped and undoped TiO_2 nanostructured thin films under UV and vis-lights, J. Hazard. Mater. 140 (2007) 69–74.
[22] J. Shang, Yao.F W.Q., Zhu.F Y.F., Wu.F N.Z., Structure and photocatalytic performances of glass/SnO_2/TiO_2 interface composite film, Appl. Catal. A 257 (2004) 25–32.